Chemical Engineering Journal 483 (2024) 149292

Contents lists available at ScienceDirect

Chemical Engineering Journal

journal homepage: www.elsevier.com/locate/cej

Photon Density Wave spectroscopy to monitor the particle size in seeded semibatch emulsion copolymerization reactions

Usue Olatz Aspiazu, Maria Paulis *, Jose Ramon Leiza *

POLYMAT, Kimika Aplikatua saila, Kimika Fakultatea, University of the Basque Country UPV/EHU, Joxe Mari Korta zentroa, 20018 Donostia-San Sebastián, Spain

A B S T R A C T

The performance of Photon Density Wave spectroscopy (PDW) is assessed to inline monitor the particle size during the seeded semibatch emulsion copolymerizations of methyl methacrylate, butyl acrylate, methacrylic acid (MMA/BA/MAA = 51/47/2 wt% composition) with particle size and solids content ranges relevant in industrial formulations. Moreover, the suitability of the technique to early detect some of the most probable deviations, such as particle aggregation and secondary nucleation, is studied. It is shown that the PDW can be successfully used to inline monitor the reduced scattering coefficient, and consequently the particle size evolution in emulsion polymerization reactions for a broad range of particle sizes and solids contents. Nevertheless, for particle sizes higher than 350 nm and solids content above 40 %, the low signal to noise ratio together with the characteristic multiple solutions regime of the theoretical reduced scattering versus the particle size curve, produces uncertainties in the determination of the particle size by PDW.

1. Introduction

Particle size and particle size distribution are important properties of polymer latexes because they strongly affect the film formation and the rheological properties of the latexes. Thus, monitoring the particle size is of paramount importance during the production of waterborne polymeric dispersions, for which real time online/inline measurements of the particle size are required.

Photon Density Wave spectroscopy (PDW), based on photon transport theory (incorporating multiple scattering), Mie theory and theory of time dependent light scattering, determines the absorption and scattering properties of highly turbid samples, what allows a dilution free particle size determination, by the introduction of a probe directly in the non-diluted samples [1–4]. A summary of the PDW theory can be found in the Supporting Information and elsewhere [4].

PDW has been used in the last decade for monitoring the particle size of a range of different processes dealing with highly turbid media. Zimmerman et al. reported the suitability of the PDW for titania particle syntheses analysis [5], while Häne et al. used the PDW to monitor the zeolite particles synthesis [6]. Münzberg et al. investigated the use of PDW to monitor the formation of formazine from different starting points and at different conditions [7]. Moreover, Reich et al. monitored an emulsification process of oil-in-water using SDS as surfactant [8]. Some bio processes were also analyzed by Hass et al. For this aim, different kind of milks were analyzed as a starting point and once the suitability of the technique for bio products was tested, beer, blood and other processes were also analyzed, such as the enzymatic decomposition of the beer at 67 °C or the oxygenation process of the blood, among others [9]. Tanguchi et al. also analyzed the suitability of PDW to detect aggregation and other phenomenon in milk samples [10]. Vargas et al. addressed the ability of PDW to monitor the fat phase transition of the fresh milk [11] and Hartwig et al. its use to detect lactose crystallization [12]. The ability of the technique to analyze cell cultivation processes in photobioreaction was also tested by Sandmann et al. [13] and its application in bioengineering was reported by Gutschmann et al. [14].

Regarding the suitability of the PDW to analyze polymerization reactions, several works can be found in literature. Hass et al. monitored the synthesis of polyacrylate nanoparticles (50 % of styrene and 50 % of other acrylics) during starved feed polymerization, with different amount of emulsifiers and particle sizes up to 200 nm at 40 % solids content (SC) in a 25 L reactor [15]. Hass et al. also analyzed the possibility of using PDW to inline monitor the particle size of several polymers such as PS, PMMA and P-*tert*-BuMA in their industrial application [16]. Particle sizes up to 350 nm and SC up to 30 % were analyzed by the authors. The formation of solvent borne acrylic copolymers obtained by the acetone process was also studied for an acrylic copolymer with high acrylic acid (AA) content by Kutlug et al. [17]. During the study the water feed and the solvent removal were analyzed. Schlappa et al. monitored the synthesis of polyvinyl acetate

* Corresponding authors.
E-mail addresses: maria.paulis@ehu.eus (M. Paulis), jrleiza@ehu.eus (J.R. Leiza).

https://doi.org/10.1016/j.cej.2024.149292
Received 26 September 2023; Received in revised form 25 January 2024; Accepted 31 January 2024
Available online 3 February 2024

Table 1
Reactions performed to evaluate the PDW.

Reaction	SC seed /%	d_p seed* /nm	PDI seed	SC targeted /%	d_p targeted /nm	Feeding time /min
R1	2.73	45	0.08	45	175	180
R2	0.3	45	0.08	40	350	180
R3	7.54	175	0.012	40	425	180
R4	3	45	0.08	40	80 / 350	240
Aggregation	33	119	0.05	–	–	65

* All particle sizes are number-average particle sizes measured by DLS using the cumulants method.

emulsions at solids contents up to 54 % (final latexes with SC from 40 to 54 % were synthesized), where only the reduced scattering coefficient was reported, due to the large discrepancies as compared with DLS in particle size calculations [18]. In a recent publication [19], they attributed the particle size calculation errors by PDW to the water-swelling of polyvinyl acetate particles stabilized with polyvinyl alcohol. Furthermore, the ability of PDW to monitor solids contents up to 70 % was also studied by Jacob et al. [20,21]. These high solids content analyzed by Jacob et al. were obtained by seeded semibatch emulsion polymerization processes with different stages and for particle sizes up to 300 nm. For particle sizes over 300 nm, agglomeration was observed and ultrasound treatment was needed [21]. Although the reaction faced some problems, PDW was able to detect the agglomeration process. This reaction was scaled up to 100 L reactor [20]. Although the reproducibility of the reaction was challenging due to its tendency to agglomerate, large particle sizes and high solids contents were analyzed and good reproducibility of the experiment and PDW data was achieved. All the mentioned analysis were carried out for monomodal dispersions. Bimodal dispersions have been also studied, but its real time monitoring was not proven, due to the high number of unknown parameters to be considered [22].

As discussed above, the suitability of PDW to analyze several materials has been tested during the last years, from ceramics to polymers, under different conditions of size and synthesis methods and getting promising results. Nevertheless, there are not in depth assessments of the monitoring of emulsion polymerization reactions covering a broad range of particle sizes and solids content during semibatch operation. Note that, the turbidity of a sample is related not only to the particle size of the dispersed phase, but also to the solids content of the medium [23]. Thus, to study the suitability of PDW to monitor particle size in emulsion polymerization processes, a wide range of particle sizes (d_p) and SC samples have to be analyzed. This way, the ability of the technique to measure the particle size at different turbidities can be studied and the limitations can be addressed. Therefore, the objective of this work is to assess PDW as an inline monitoring sensor in emulsion polymerization processes under conditions typically used in industrial production plants; specifically, seeded semibatch emulsion polymerizations of acrylic monomers. Moreover, the suitability of the PDW to detect different phenomena that can occur during emulsion polymerization reactions will also be studied; namely, the aggregation/coagulation processes and the creation of new polymer particles.

2. Experimental section

2.1. Materials

Methyl methacrylate (MMA) (Quimidroga), n-butyl acrylate (BA) (Quimidroga) and methacrylic acid (MAA) (Aldrich) were used as received. Sodium Dodecyl Sulphate (SDS, Aldrich) was used as emulsifier. Dowfax 2A1 was kindly supplied by Dow Chemical and used as emulsifier. Ammonium Persulfate (APS, Aldrich) was used as initiator. Deionized high-purity water obtained through a Merck Millipore system (DI-water) was used as continuous medium in the emulsion polymerizations and to dilute the samples for DLS analysis (water conductivity was lower than 1μS/cm in all cases) and hydroquinone (Aldrich) was used as inhibitor to stop the reaction in the samples withdrawn from the reactor for offline analysis.

2.2. Synthesis of latexes monitored by PDW

Seeded semibatch emulsion polymerization reactions were monitored using the PDW equipment. First a seed was synthesized and then the particles of the seed were grown until the targeted particle size (this step was monitored with the PDW). A seed with target molar

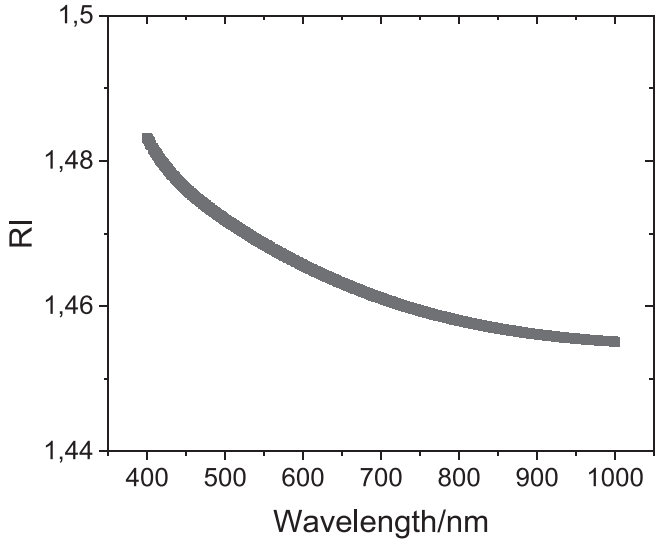

Fig. 1. Calculated evolution of the refractive index over the wavelength for the terpolymer of MMA/BA/MAA with a weight composition of 51/47/2 %.

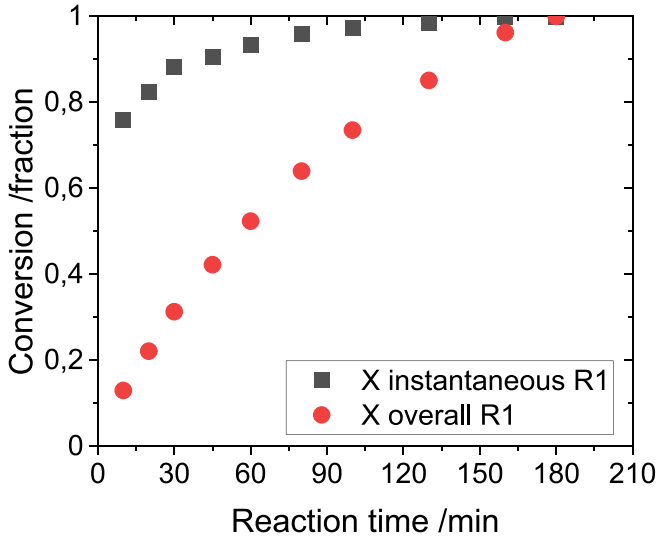

Fig. 2. Evolution of the instantaneous and overall conversions of experiment R1.

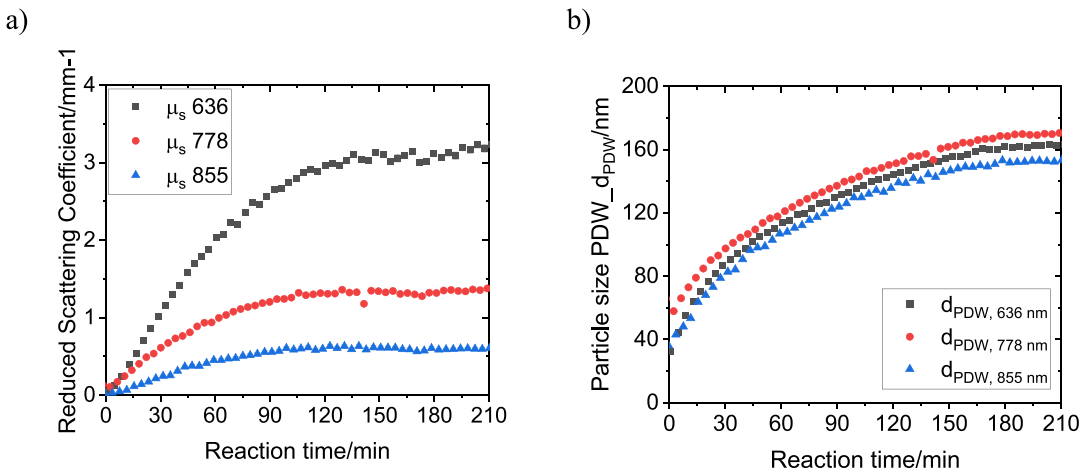

Fig. 3. Inline monitoring of particle size by PDW in experiment R1: a) Inline reduced scattering coefficient evolution, and b) particle size evolution for each of the laser wavelength.

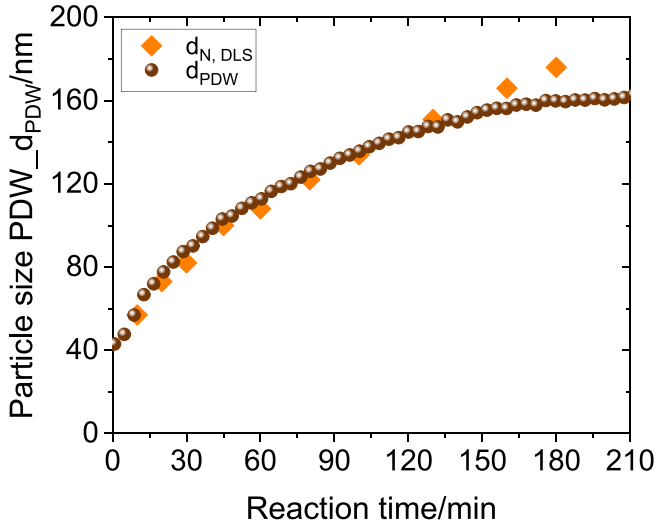

Fig. 4. Inline monitoring of particle size by PDW in experiment R1. Average particle size evolution obtained by PDW compared to the number-average particle size obtained by offline DLS.

compositions of MMA/BA 50/50 was synthesised by batch emulsion polymerization. For that, water, comonomers and emulsifier were mixed in the reactor. Once all the mixture was heated to 85 °C, a shot of initiator was added. The mixture was left to react for 4 h. The recipe for the synthesis of the seed is presented in the Supporting Information Table SI 1.

The seeded semibatch emulsion polymerization reactions were performed as follows: First, the seed was loaded in the reactor and it was diluted to reach the needed solids content between 0.3 and 8 %, depending on the initial and targeted particle sizes. Then, the mixture was heated to reach the reaction temperature (85 °C). Subsequently, monomers and initiator were fed to the reactor in two feeding streams during 180 min at constant flow rate for R1-3 reactions. The recipes for the reactions are presented in the Supporting Information Table SI 2. After the feeding, the latex was maintained at the reaction temperature for 30 min to remove the residual monomer.

For mimicking the formation of new polymer particles (i.e., secondary nuclations) (R4 reaction), a shot of seed particles was introduced during the monomer feeding stage in a seeded semibatch emulsion polymerization (recipe in the Supporting Information Table SI 2). This is a typical strategy used to produce high solids low viscosity latexes in the production of waterborne polymer dispersions [24–29]. Therefore, a preformed seed with 0.3 % of solids content and a particle size of 45 nm was heated to 85 °C, the reaction temperature, and the monomers were directly fed over the seed for 240 min. To mimick the formation of a new crop of particles, and hence a bimodal PSD, after 142 min of feeding, a shot of the seed latex (45 nm particles) was injected to the reactor. The particle growth during the 240 min of feeding and the 30 min of postpolymerization was monitored by PDW.

All these reactions were carried out in a 1 L calorimeter reactor (RC1e) from Mettler Toledo, equipped with a jacketed glass reactor fitted with a sampling device, a nitrogen inlet, feeding inlets, a Pt-100 probe, the PDW probe and a stainless steel anchor type stirrer (for more details see Supporting Information). Reaction temperature and inlet flow rates of semicontinuous feeds were controlled by an automatic control system, iControl RC1e Software. In all the reactions, samples were withdrawn every 10–15 min during the first 60 min of the reaction and every 20–30 min after that time to analyse the evolution of monomer conversion and particle size offline by DLS. Detailed information about the sampling (amount, time, extracted mass) in all reactions and the reproducibility of PDW results can be found in the Supporting Information as well.

For the aggregation detection test, a sodium chloride solution was prepared with different salt concentrations (0.05 and 0.15 M). These solutions were fed to a preformed latex of 33 % of SC and a particle size of 119 nm during 65 min and with a speed of 1 g/min. The aggregation detection test was carried out in a 0.5 L beaker equipped with a magnetic stirrer, a feeding inlet and the PDW probe. The reaction was performed at room temperature and the addition of the salt solution was done with a burette.

A summary of the conditions of the reactions including solids content (SC) and seed and targeted particle diameters, as well as feeding times are presented in Table 1.

2.3. Characterization

2.3.1. Conversion calculations

As samples were withdrawn from the reactor to measure particle size by DLS, conversions were measured by gravimetric analysis. The instantaneous conversion is defined as the amount of polymer produced divided by the mass of monomers fed until the sampling time (Eq. (1)). The overall conversion is the amount of polymer divided by the total amount of monomer in the formulation (Eq. (2)).

$$Xa\ instant = \frac{Polymerized\ monomer\ (t)}{Total\ fed\ monomer\ (t)} \quad (1)$$

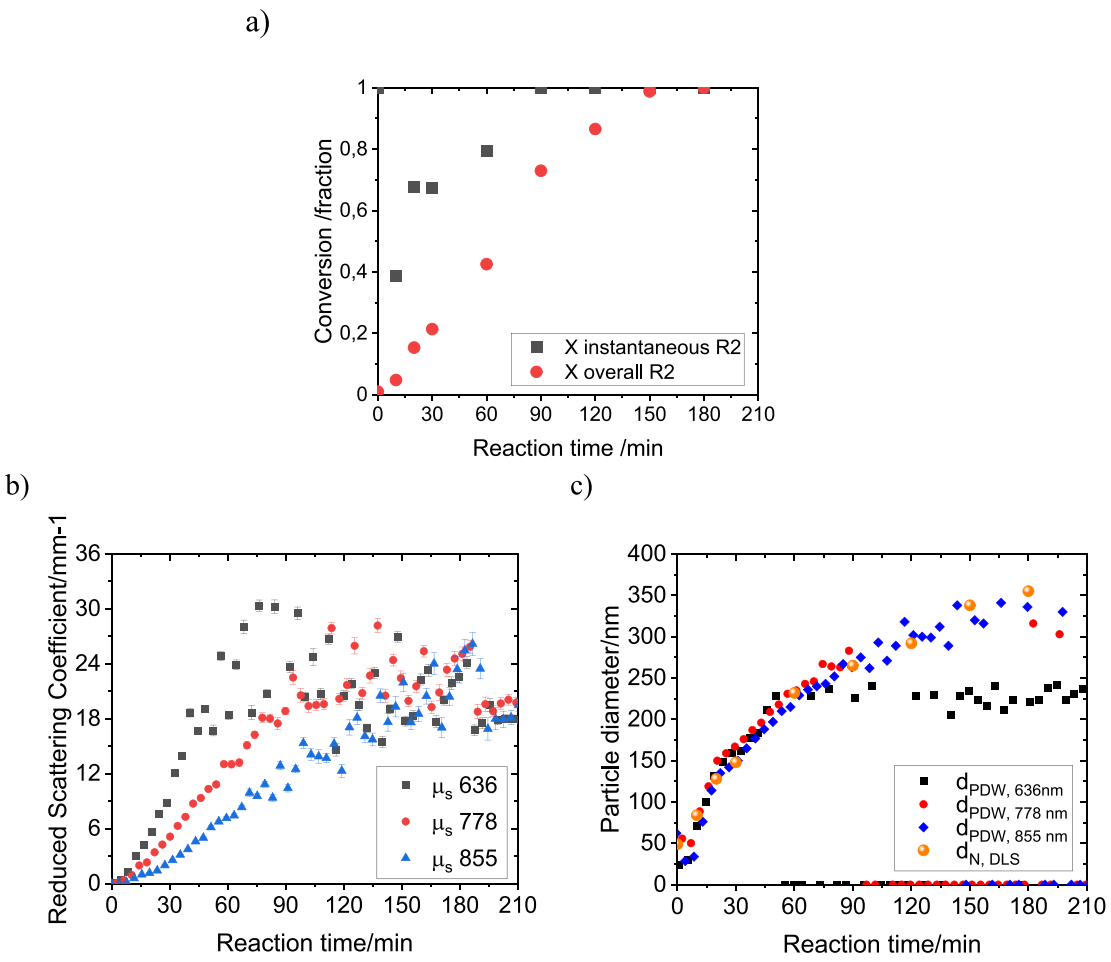

Fig. 5. Inline monitoring of particle size by PDW in reaction R2: a) evolution of instantaneous and overall conversions, b) reduced scattering coefficient evolution, and c) particle size evolution for each of the laser wavelength.

$$Xa\,overall = \frac{Polymerized\ monomer\ (t)}{Total\ monomer\ (end\ of\ reaction)} \quad (2)$$

Note that conversions can be also calculated from the heat of reaction measured by the calorimetric reactor. A comparison of the overall conversions measured by both methods as well as the heat released during the polymerization for reaction R1 are included in the Supporting Information.

2.3.2. Photon Density Wave spectroscopy

A Photon Density Wave spectrometer developed by PDW Analytics GmbH (PDWA) (Potsdam, Germany) was used for the particle size monitoring [1,18,21]. The Photon Density Wave spectrometer was equipped with four lasers of 636, 778, 855 and 973 nm wavelengths, 27 possible distances from 3 to 25 mm and 41 possible frequencies from 10 to 610 MHz. To calculate the particle size a software developed by innoFSPEC department from the University of Potsdam was used, based on Mie-Theory and the theory of dependent scattering. To calculate the particle size the refractive indices of the continuous and dispersed phase (shown below), as well as the volume fraction of the dispersed phase are needed.

2.3.3. Dynamic light scattering

A Zetasizer Nano Series (Malvern Instrument) dynamic light scattering (DLS) was used as reference technique in this work. For the analysis, the latex was diluted in DI-water until an attenuation number of 6–7 was achieved at 4.65 mm position and a PDI value below 0.1 was obtained, to ensure single scattering conditions. DLS measurements were carried out at room temperature and three repeated measurements were carried out for each sample. All reference particle sizes shown in this section are number-average particle sizes measured by DLS, except for reaction R4, where intensity-average particle sizes are also reported.

2.3.4. Capillary hydrodynamic fractionation (CHDF)

Particle size distributions were obtained by capillary hydrodynamic fractionation. A CHDF3000 instrument (Matec Applied Sciences) was used for the analysis, with its proprietary CHDF3000 PDA 2.1 software and C-204 column (internal diameter 20 μm). The samples were diluted in carrier fluid (Matec Applied Sciences) to 0.05 % SC and the measurements were done at a flow rate of 1.4 mL/min at 35 °C.

2.3.5. Refractive index measurement

The refractive index of the terpolymer of MMA/BA/MAA with weight composition of 51/47/2 % was experimentally measured. For that, an experimental method developed by Hass et al. [2] was used. By measuring the refractive index of a liquid dispersion of the polymer $n_{dispersion}(\lambda)$ as a function of wavelength and volume fraction of the dispersed phase, φ, Eq. (3) allows for the extrapolation of the refractive index of the pure material by global analysis:

$$n_{disp.\ phase}(\lambda) = \left[\frac{n^2_{dispersion}(\lambda) + n^2_{cont.\ phase}(\lambda)[\varphi - 1]}{\varphi}\right]^{1/2} \quad (3)$$

The spectral interpolation of the refractive index is achieved based on a Cauchy polynomial. Fig. 1 shows the calculated refractive index over the wavelengths for the synthesised terpolymer of MMA/BA/MAA

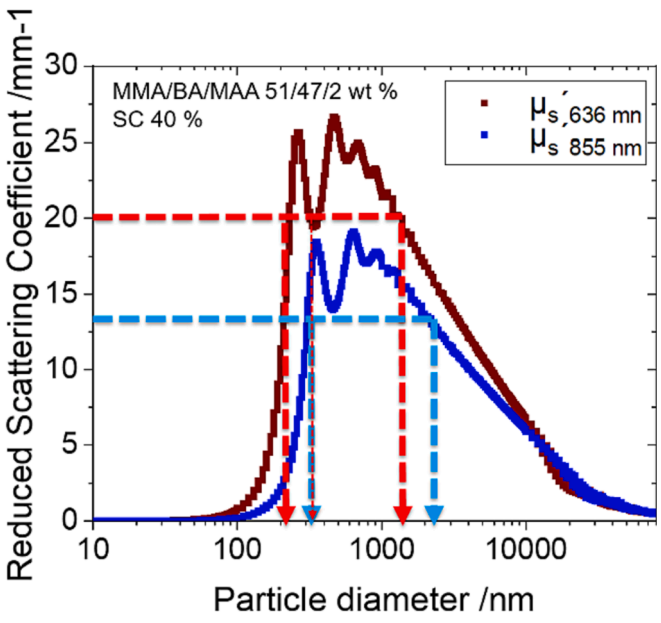

Fig. 6. Theoretical dependence of the reduced scattering coefficient on the particle size for a monodispersed dispersion of spherical particles with 40 % of SC for two wavelengths (636 and 855 nm, dark red and dark blue lines, respectively). Dashed light red and dashed light blue lines show the experimentally obtained reduced scattering coefficient value for the final latex of R2 experiment measured with 636 and 855 nm wavelengths, respectively. See text for the discussion on the lines drawn in the plot. (For interpretation of the references to colour in this figure legend, the reader is referred to the web version of this article.)

with a weight composition of 51/47/2 %.

3. Results and discussion

3.1. Inline monitoring of particle size in semibatch emulsion polymerization: Effect of particle size and solids content range

Three seeded semibatch emulsion copolymerization (MMA/BA/MAA: 51/47/2 wt%) reactions were used to assess the performance of the PDW; specifically, reactions R1, R2 and R3.

Reaction R1 aims to produce a latex with an average particle size of 175 nm and a solids content of 45 wt% starting from a seed (S1, see Supporting Information) with a particle size of 45 nm. Fig. 2 presents the evolution of the instantaneous and overall conversions for this experiment, which indicates that the reaction proceeded under starved conditions with instantaneous conversions above 90 % during almost the whole reaction; which means that the concentration of comonomers in the polymer particles was low and it was maintained relatively constant during the whole reaction.

Fig. 3a shows the inline reduced scattering coefficient evolution for reaction R1 monitored by the lasers with 636, 778 and 855 nm wavelengths. As can be seen, the reduced scattering coefficient increases as the reaction proceeds due to the increase in the particle size and the solids content during the monomer feeding stage of the semibatch process. Moreover, the higher the wavelength used to perform the analysis, the lower is its sensitivity to the changes that are occurring in the reactor. Note that although the probe used had a laser at higher wavelength, $\lambda = 973$ mn, the signal to noise ratio was too low and hence it has not been included in the figure. From the reduced scattering coefficient evolution, the particle size was retrieved, as shown in Fig. 3b (see Supporting Information for details on the particle size calculations). As can be seen, a different particle size is obtained for each wavelength. The scattered light depends on the wavelength of the emitted light and hence the different particle sizes obtained do represent the broadness of the distribution of the latex samples analysed during the reaction.

An average diameter can be computed from the values calculated at each laser wavelength and the value obtained as well as the offline value obtained by DLS are presented in Fig. 4. There is a very good agreement (differences lower than 10 %, see Supporting Information) between the inline average particle size obtained by PDW and the offline number-average value measured by DLS. Therefore, it can be said, that the synthesis of MMA/BA/MAA polymer particles by seeded semibatch emulsion polymerization up to 175 nm and 45 % SC was properly monitored by PDW.

In reaction R2, a broader evolution of the particle size was assessed. The reaction started with the same seed latex as R1 (but substantially more diluted) and the final particle size targeted was 350 nm with a solids content of 40 wt%. Fig. 5a shows the evolution of the instantaneous and overall conversions. In this case, an inhibition period of 30 min can be observed at the beginning of the reaction, but after that, the polymerization proceeded under starved conditions. Fig. 5b presents the evolution of the inline measurements of the reduced scattering. Notably the reduced scattering coefficient values are substantially higher than

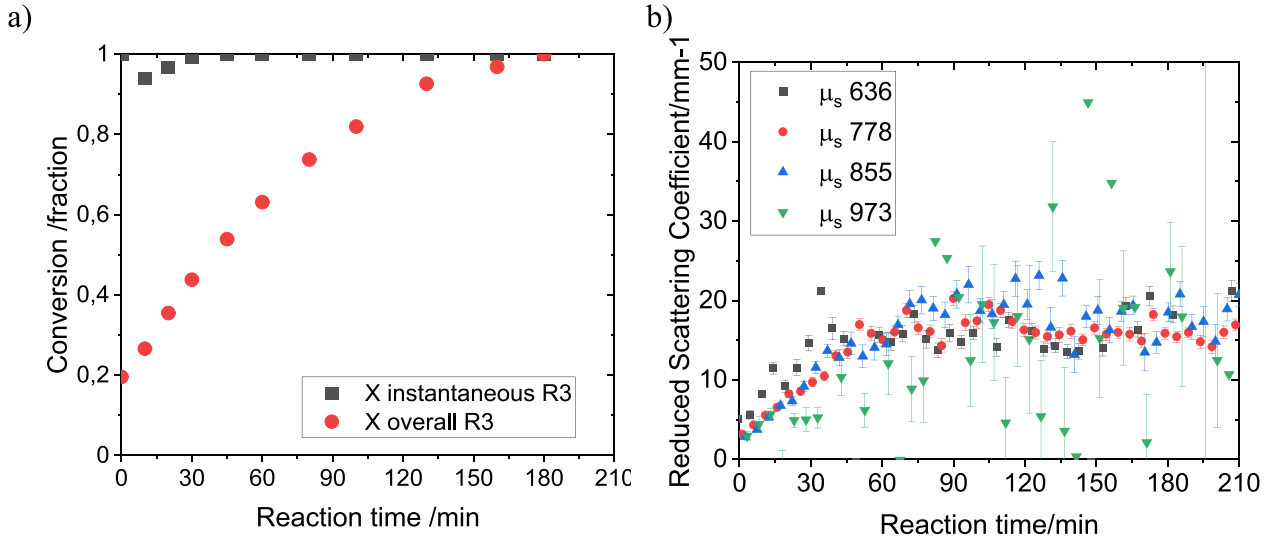

Fig. 7. Inline monitoring of particle size by PDW in reaction R3. a) Evolution of instantaneous and overall conversions, b) evolution of the reduced scattering coefficient during the entire reaction.

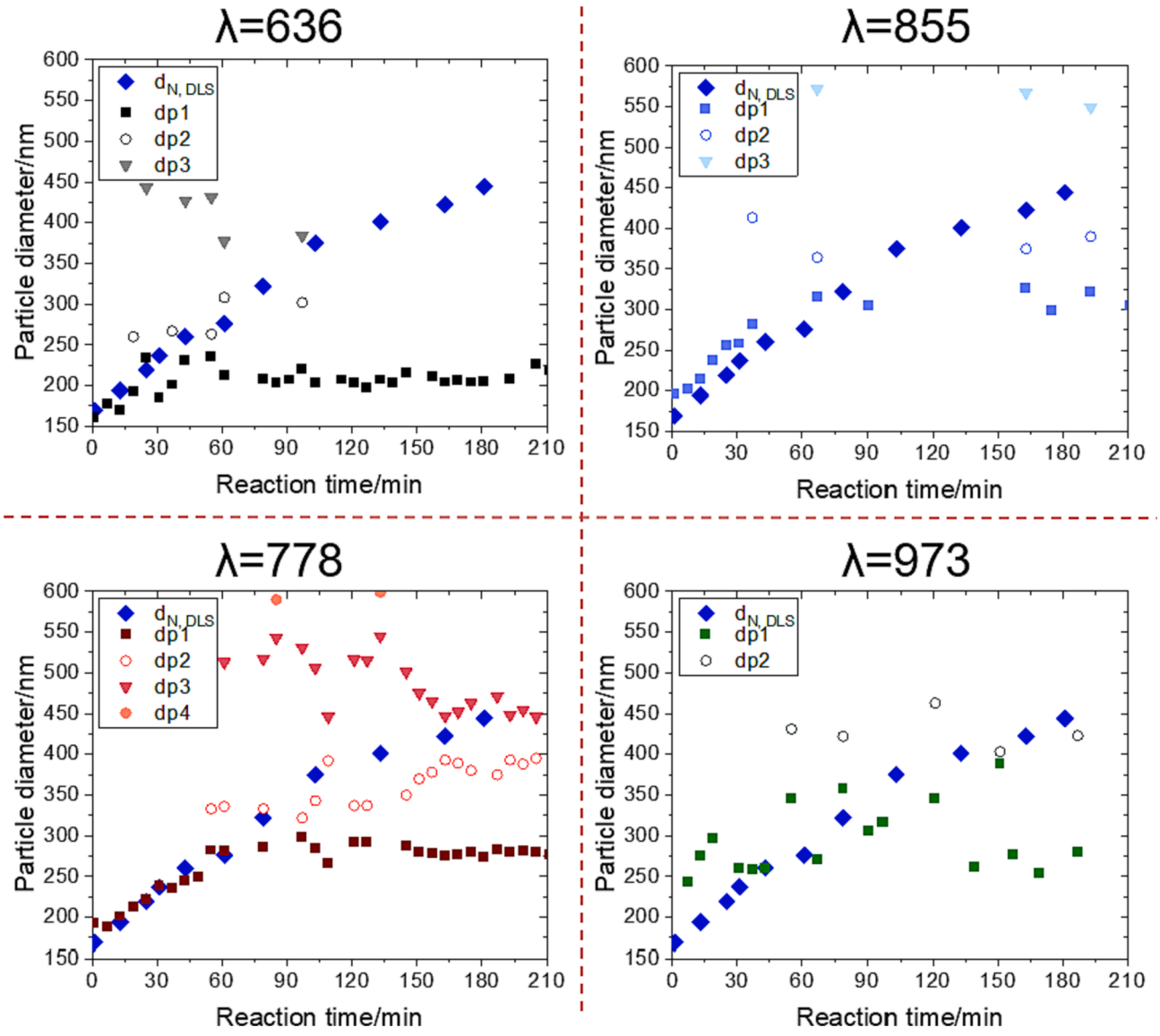

Fig. 8. Particle size evolution for each wavelengths (636, 778, 855 and 973 nm) during the inline monitoring of reaction R3 by PDW.

those measured for reaction R1 for the three wavelengths, indicating a faster growth of the seed particles (see Fig. 5c). However, the scatter of the reduced scattering measurement increased with reaction time and furthermore the lower the wavelength, the higher the scatter. Interestingly, above 120 min of reaction the reduced scattering values for all wavelengths were high and mostly overlapped. The particle sizes retrieved from the reduced scattering values at each wavelength are presented in Fig. 5c, which initially match perfectly with the DLS data (up to 60 min). However, in order to understand the evolution of the particle size obtained by PDW from that point on, the theory behind PDW should be further considered.

Fig. 6 shows the theoretical dependence of the reduced scattering coefficient over the particle size for a monodispersed latex of MMA/BA/MAA 51/47/2 wt% composition and 40 % of solids content. As can be seen, in a broad range of particle sizes (note that in Fig. 6 particle size spans from few nanometers to several microns) the reduced scattering shows different regimes. At small particle sizes (the limit depends on the wavelength of the laser used), there is an increase of the reduced scattering with the increase of the particle size. At intermediate particle sizes, the reduced scattering reaches an oscillating plateau; namely, the reduced scattering is similar for a broad range of particle sizes (up to few microns). In the third regime, further increasing the particle size the reduced scattering decreases and the values at different wavelengths tend to overlap. Interestingly, the end of the first regime is reached at smaller particle sizes, the smaller is the wavelength of the laser (250 nm at 636 nm and circa 350 nm at 855 nm).

The particle size is retrieved from the experimentally measured reduced scattering coefficient using the theoretical relationship plotted in Fig. 6 for the optical properties of the sample analysed (see Supporting Information). This means that in a blind analysis, multiple solutions are expected for a given measured reduced scattering value (see dashed lines intercepting in the curves). Therefore, to obtain a unique value of particle size the PDW analysis must be done at least at two wavelengths as shown in Fig. 6, expecting a solution that is equal for the measurement done in the two wavelengths (see Supporting Information Figure SI2).

On the other hand, if one has certain knowledge about the sample like in this case, where emulsion polymerization reactions are considered and the expected particle size should be submicron, one can limit the maximum particle size and hence limit the ambiguity. In practice, however, and as observed in the particle sizes retrieved in reaction R1, the particle sizes retrieved are not exactly the same because of the dispersity of the samples. Anyhow, from the particle size gathered an average value (PDW average) can be calculated.

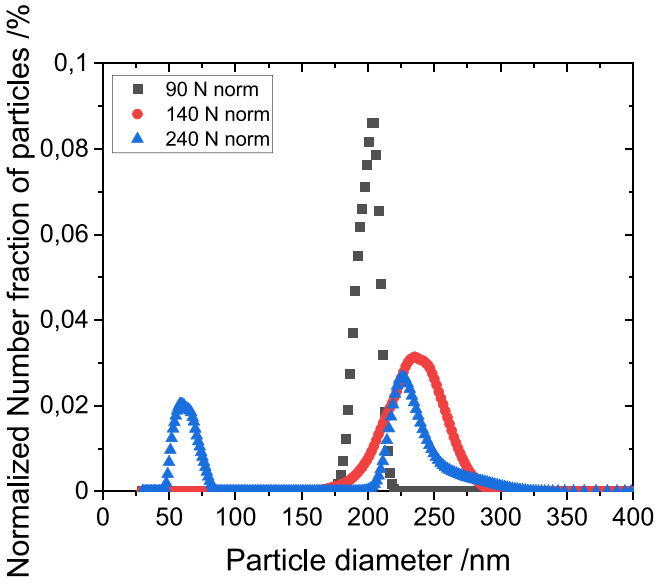

Fig. 9. Normalized number average particle size distribution evolution measured by CHDF during reaction R4, after 90, 140 and 240 minutes of reaction.

Nonetheless, experiment R2 brought another limitation of the technique. This is the fact that, even in the submicron region, the reduced scattering coefficient can be in the second regime, where there is multiplicity of solutions for a given reduced scattering value. As discussed above, this multiple solution regime is reached at smaller particle sizes the smaller is the wavelength of the laser employed (see Supporting Information Figure SI2 and Figure SI3 for more insight). This explains that for wavelength 636 nm, reliable results were only obtained till 60 min of reaction (see Fig. 5c and Fig. 6), whereas the whole reaction was monitored for the 855 nm wavelength.

Fig. 6 shows the particle size retrieved from the theoretical dependence curve of the reduced scattering coefficient for the final latex of R2 experiment at 636 and 855 nm wavelengths. As can be seen, the reduced scattering value obtained for 636 nm is in the multiple solution regime (light red line), which gives four possible solutions (232, 317, 369 and 1245 nm), while for 855 nm (light blue line) only two possible solutions would be possible (306 and 2171 nm). As can be observed, the 317 and 306 nm are the closest ones, which are also close to the DLS value, 355 nm.

Therefore, it can be seen in Fig. 5c that the inline values measured at 855 nm by PDW are in very good agreement with the DLS values (differences lower than 10 %, see Supporting Information). The inline values gathered at the lower wavelengths only overlapped up to the regions where the reduced scattering coefficient was in the first regime, suggesting that just the first particle size result was given by the PDW.

Therefore, in the third reaction, as a larger particle size was targeted, the laser of 973 nm wavelength was incorporated to the PDW analysis. Reaction R3 was designed to produce an acrylic copolymer latex with 425 nm and 40 wt% solids content. The seed latex (the latex synthesized in reaction R1) had a particle size of 175 nm and it was diluted to 7.5 wt %.

Fig. 7a shows that the polymerization proceeded under starved conditions during the entire experiment; namely, with monomer concentration relatively low in the polymer particles and mostly constant during the feeding period. Fig. 7b presents the evolution of the reduced scattering coefficient during the whole process. Contrary to what was observed in the previous two experiments (R1 and R2), in this experiment the reduced scattering coefficients are in the plateau region (multiple solution regime) almost from the very beginning of the reaction.

As can be seen in Fig. 7b, in the first 40 min, where the reduced scattering coefficient increases with reaction time (or particle size), the difference in the reduced scattering with the wavelength are less clear than in experiments R1 and R2. This is due to a lack of signal that comes from the probe configuration used in this work. As multiple scattering conditions are analysed, the intensity of the light decreases with the distance from the emission point, and if the light is lost before reaching the detection fiber (more probable at higher particle size and solids content conditions), noise is measured in the detection point. If the probe was built with other distances (with smaller emission/detection distances in this specific case), the quality (signal to noise ratio) of the measured data would have improved. This means that the configuration of the emission/detection fiber distances in the probe can be optimized for each expected evolution of the particle size. In other words, the probe configuration included in the current PDW set-up is not universal.

After the first 40 min, all data start to overlap. The 778 and the 855 wavelengths continue to increase a bit, due to their capacity to analyse higher turbidity conditions, but after 60 min of reaction, all wavelength reach the multiple solution regime and all data is overlapped. At this point, each reduced scattering data corresponds to more than one

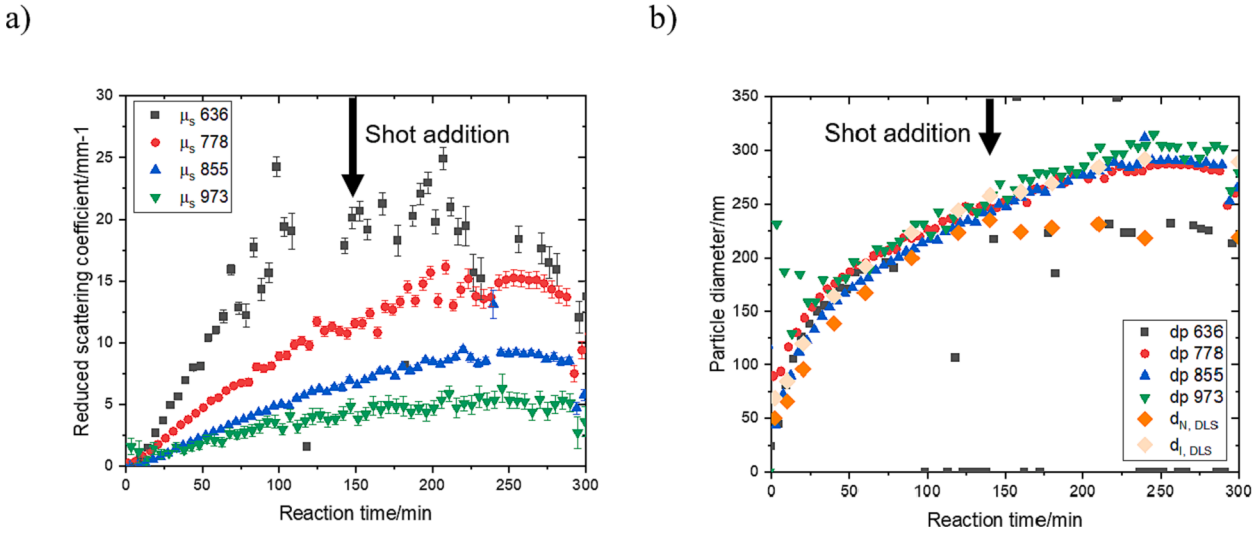

Fig. 10. Inline monitoring of particle size in experiment R4: a) Inline reduced scattering coefficient evolution results and b) particle size evolution retrieved from the reduced scattering coefficient and offline measured by DLS.

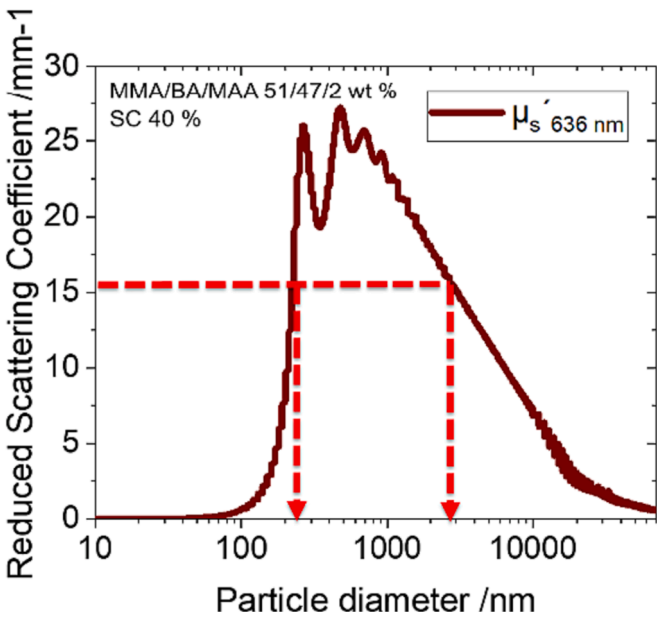

Fig. 11. Theoretical dependence of the reduced scattering coefficient on the particle size for a monodispersed dispersion of spherical particles with 40 % of SC at 636 nm wavelength and polymer composition of MMA/BA/MAA 51/47/2 wt% (dark red). Light red dashed line represents the experimentally measured reduced scattering coefficient value at the end of R4 experiment, 15.5 mm^{-1}. (For interpretation of the references to colour in this figure legend, the reader is referred to the web version of this article.)

possible particle size. Thus, to calculate the real particle size, the different solutions retrieved from each wavelength where compared between them and to the particle size measured offline by DLS (Fig. 8).

As can be seen in Fig. 8, with the smallest wavelength (636 nm) the reaction can only be monitored for the first 40 min, up to a particle size of about 250 nm. For the rest of the reaction, the reduced scattering value is in the multiple solution regime, thus the particle size cannot be directly retrieved. For the second wavelength (778 nm), considering all the possible particle size solutions, almost all the reaction can be monitored, but, selecting the correct particle size is very challenging, since the comparison with other wavelengths is very difficult to apply, due to the polydispersity of the samples. For the third wavelength (855 nm), a substantial part of the reaction can also be monitored. There is a time region where the particle size could not be retrieved due to very low signal to noise ratio in the measured data. For the highest wavelength (973 nm) even if the reduced scattering coefficient seems to be relatively constant, the error of the measurement is too big compared to the other wavelengths and the signal to noise ratio is too low to reliably retrieve the current particle size.

As can be seen, considering all the possible diameters, there is always one that fits the data obtained from the DLS. Nevertheless, the correct selection of the diameter is very challenging. After these observations it can be concluded that there are several reasons why all wavelengths show certain limitations, which are related to the settings of the PDW probe that have been used in this work. For the smallest wavelengths (636, 778 and 855 nm), the sensitivity to the turbidity of the medium is too high and multiple solution regime is reached in polymerization with rapid increase of particle size and solids content. For the biggest wavelength (973 nm), there are not enough short distances to get accurate signals with a high signal to noise ratio. To overcome these problems, the configuration of the laser fibers in the probe should be modified.

3.2. Inline monitoring of bimodal PSD by PDW

The suitability of PDW to detect secondary nucleations that might create bimodal PSD was assessed in this section. Secondary nucleation is sometimes desired in order to generate a bimodal latex because this allows increasing solids content with little or low impact on the viscosity of the dispersion [25]. However, other times secondary nucleations are not desired and they might be an indication of a deviation of the target growth of the particles originated from a failure in the feeding of surfactant, initiator or even monomer. In any case, early detection of the formation of a new crop of polymer particles during an emulsion polymerization process is desired.

Reaction R4 was carried out to mimick the generation of a new

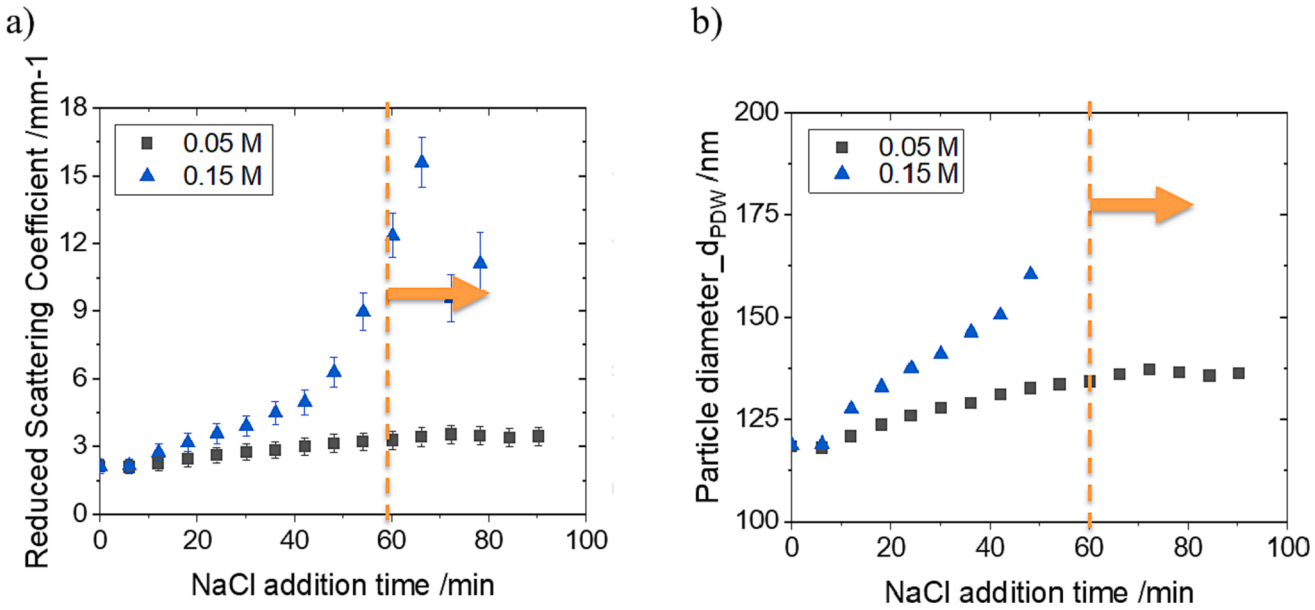

Fig. 12. Polymer particle aggregation detection test. a) Inline reduced scattering coefficient (636 nm wavelength) evolution and b) particle size evolution, during the aggregation experiment for two different salt concentrations: 0.05 M in black and 0.15 M in blue. The orange line represents the moment were the coagulation becomes massive for the case of 0.15 M NaCl addition. (For interpretation of the references to colour in this figure legend, the reader is referred to the web version of this article.)

population of small particles during a seeded semibatch polymerization process. This reaction started with a seed latex with a particle size of 45 nm and a target particle size of 350 nm, like in experiment R2. However, at an intermediate point during the feeding of the monomer (at 142 min), an amount of the same seed latex was injected to the reactor to create the bimodal latex.

PDW was used to monitor inline the emulsion polymerization. Furthermore, in addition to offline DLS analysis, this time samples were also analysed by CHDF (Capillary HydroDynamic Fractionation), because bimodal or multimodal population are better detected by this chromatographic technique than with DLS [30]. Fig. 9 presents the normalized number-average particle size distributions measured by CHDF of the samples withdrawn from the reactor at different reaction times (90, 140 and 240 min) (normalized weight-average particle size distribution can be found in the Supporting Information). It was confirmed that up to 140 min, a growing monomodal particle size distribution was present in the reactor, whereas at the end of the reaction a bimodal latex was clearly observed.

Fig. 10a presents the inline evolution of the reduced scattering coefficient at each of the wavelengths of the probe. At the lowest wavelength (636 nm) the reduced scattering coefficient increases linearly up to around 100 min, where a plateau value is achieved which is maintained after the shot of the seed latex to start decreasing at the end of the feeding of the monomers. The trend for the other wavelengths is similar, the reduced scattering coefficient increases linearly up to 240 min of reaction to reach a plateau value (the value is higher the lower is the wavelength) with almost no noticeable effect of the shot of the seed latex.

According to the discussion before, this reduced scattering evolution should allow to calculate a single particle size for all the wavelengths during almost the whole polymerization reaction. Fig. 10b displays the particle sizes retrieved from the reduced scattering values and the offline values measured by DLS. Note that two averages, number and intensity based ones, are plotted for the DLS measurements. The DLS particle sizes (both averages) increase up to the point the seed shot is injected (142 min). Beyond this time the two averages diverge, indicating, as shown by the CHDF measurements in Fig. 9, that a bimodal latex has been formed. Since DLS is unable to distinguish the two populations, the average values diverge into higher sizes (for $d_{I,DLS}$) and smaller ones (for $d_{N,DLS}$). Interestingly, the inline particle size values measured by PDW for the highest wavelengths (778, 855 and 973 nm) seem to follow closer the intensity-average values during the whole process. On the contrary, for the smallest wavelength (636 nm) a different behaviour is appreciated. The value obtained from the smallest wavelength agrees with the number-average particle size of the DLS, the one showing the effect of the added particles. This is also shown when studying how the Mie curve and the experimental value of the reduced scattering coefficient intercept.

Fig. 11 shows how the experimentally measured reduced scattering coefficient at 636 nm at the end of R4 reaction (15.5 mm^{-1}) is intercepting the theoretical curve in the first regime (linear regime). Thus, it can be concluded that even if for the highest wavelengths there is no noticeable change in the measured size detected after the shot of the seed latex, the smallest wavelength seems to be more sensitive to the scattering of the small particles than to the large ones.

3.3. Detection of aggregation of polymer particles by PDW

Another important phenomenon that might occur in emulsion polymerization reactions, and that is not desired, is the aggregation or coagulation of particles that might cause important economical losses in industrial processes. Early detection of aggregation is therefore desired in industrial production of polymer latexes. In this section, the suitability of the PDW to inline detect changes in the reduced scattering (and hence particle size of the dispersion) during an aggregation process will be evaluated.

For this purpose, the stability of a preformed ionically stabilized latex was modified by the addition of a solution of salt (NaCl), and the reduced scattering coefficient and the particle size were monitored by PDW during the addition of the salt. Two salt concentrations were tested to destabilize the latex at different speeds. The latex used was a MMA/BA/MAA copolymer with a 51/47/2 wt% composition stabilized with SDS and a particle size of 119 nm and solids content of 33 wt%. The NaCl solutions employed were 0.05 M and 0.15 M. The solutions were fed to the beaker at a flow rate of 1 g/min during 65 min. The obtained results are presented in Fig. 12.

Fig. 12 displays the evolution of the reduced scattering (the scattering measured at the 636 nm wavelength is only shown) and the retrieved particle size for the two concentrations of NaCl solutions. As can be seen, for the lowest salt concentration, the coagulation was little and the particle size change was properly monitored during the entire aggregation process, to reach a final value of 137 nm. For the higher salt concentration, an exponential increase of the reduced scattering coefficient is observed after 50 min of salt addition, showing clearly the coagulation. In this second case, the entire latex was coagulated forming a solid body at 60 min, but an abnormal increase of the reduced scattering coefficient started to occur earlier (at 40–50 min). Thus, it was shown that PDW is a suitable tool to inline detect coagulation/aggregation phenomena and to early detect coagulation, leaving some time to take actions to avoid it, during emulsion polymerization reactions.

4. Conclusions

In this work, the suitability of the PDW to monitor the particle size evolution of polyacrylate latexes synthesized by semibatch emulsion polymerizations was discussed. First, a broad range of particle sizes and solids contents were analysed (from 45 to 425 nm particle size and from 0.3 to 45 % of SC, respectively) and the limits for the submicron size analysis of the described PDW equipment was shown and how this is affected by the Mie curve. The higher the wavelength, the higher the particle size that can be properly analysed. Regarding the analysed MMA/BA/MAA 51/47/2 terpolymer system, particle sizes up to 350 nm at solids contents up to 40 % were properly analysed. For particle sizes over 400 nm, multiple solution regime of the theoretical reduced scattering curve was reached for all the used wavelengths and low signal to noise values were obtained for the used distances, making challenging to retrieve the particle size in real time.

Then, the ability of the PDW to detect the formation of new nucleations and aggregation was studied, showing that the detection of new nucleations is very challenging. Nevertheless, it could be inferred from the scattering at lower wavelengths, that this wavelength is more sensitive towards secondary nucleations (636 nm). On the other hand, coagulation of polymer particles is quickly monitored, before a catastrophic reaction takes place, by inline monitoring the evolution of the reduced scattering coefficient.

CRediT authorship contribution statement

Usue Olatz Aspiazu: Methodology, Investigation, Writing – original draft, Data curation. **Maria Paulis:** Conceptualization, Funding acquisition, Supervision, Writing – review & editing. **Jose Ramon Leiza:** Conceptualization, Writing – review & editing, Funding acquisition, Supervision.

Declaration of competing interest

The authors declare that they have no known competing financial interests or personal relationships that could have appeared to influence the work reported in this paper.

Data availability

Data will be made available on request.

Acknowledgements

The authors would like to thank the financial support from the Basque Government (IT-1525-22), European Union's Horizon 2020 Research and Innovation Programme for the funding received through the NanoPAT project (grant agreement n° 862583), PDW Analytics for the PDW equipment and innoFSPEC department from Potsdam University for the training and the help during the study. Thanks also to Dr. Amaia Agirre for the CHDF analysis. Finally, special thanks to Dr. Marvin Münzberg and Sebastian Zimmerman from Potsdam University for the extensive discussions on the PDW results.

Appendix A. Supplementary data

Supplementary data to this article can be found online at https://doi.org/10.1016/j.cej.2024.149292.

References

[1] L. Bressel, R. Hass, O. Reich, Particle sizing in highly turbid dispersions by photon density wave spectroscopy, J Quant Spectrosc Radiat Transf 126 (2013) 122–129, https://doi.org/10.1016/j.jqsrt.2012.11.031.
[2] R. Hass, M. Münzberg, L. Bressel, O. Reich, Industrial applications of photon density wave spectroscopy for in-line particle sizing, Appl Opt 52 (2013) 1423–1431.
[3] L. Bressel, R. Hass, Photon Density Wave (PDW) Spectroscopy for Nano- and Microparticle Sizing, in: In Solid State Development and Processing of Pharmaceutical Molecules, 2021, pp. 271–288, https://doi.org/10.1002/9783527823048.ch4-10.
[4] L. Bressel, Bedeutung der abhängigen Streuung für die optischen Eigenschaften hochkonzentrierter Dispersionen (Significance of dependent scattering for the optical properties of highly concentrated dispersions), University of Potsdam, 2016.
[5] S. Zimmermann, O. Reich, L. Bressel, Exploitation of inline photon density wave spectroscopy for titania particle syntheses, J. Am. Ceram. Soc. 106 (1) (2023) 671–680, https://doi.org/10.1111/jace.18744.
[6] J. Häne, D. Brühwiler, A. Ecker, R. Hass, Real-time inline monitoring of zeolite synthesis by photon density wave spectroscopy, Microporous Mesoporous Mater. 288 (June) (2019) 109580, https://doi.org/10.1016/j.micromeso.2019.109580.
[7] M. Münzberg, R. Hass, N. Dinh Duc Khanh, O. Reich, Limitations of turbidity process probes and formazine as their calibration standard, Anal Bioanal Chem 409 (3) (2017) 719–728, https://doi.org/10.1007/s00216-016-9893-1.
[8] O. Reich, L. Bressel, and R. Hass, "Sensing emulsification processes by Photon Density Wave spectroscopy," *Procedings fo SPIE-the international society for Optical Engineeringhe international society for Optical Engineering*, vol. 7753, 2011.
[9] R. Hass, D. Munzke, S. Vargas Ruiz, J. Tippmann, O. Reich, Optical monitoring of chemical processes in turbid biogenic liquid dispersions by photon density wave spectroscopy, Anal Bioanal Chem 407 (10) (2015) 2791–2802, https://doi.org/10.1007/s00216-015-8513-9.
[10] J. Tanguchi, H. Murata, Y. Okamura, Analysis of aggregation and dispersion states of small particles in concentrated suspension by using diffused photon density wave spectroscopy, Colloids Surf B Biointerfaces 76 (1) (2010) 137–144, https://doi.org/10.1016/j.colsurfb.2009.10.027.
[11] S. Vargas Ruiz, R. Hass, O. Reich, Optical monitoring of milk fat phase transition within homogenized fresh milk by photon density wave spectroscopy, Int Dairy J 26 (2) (2012) 120–126, https://doi.org/10.1016/j.idairyj.2012.03.012.
[12] A. Hartwig, R. Hass, Monitoring lactose crystallization at industrially relevant concentrations by photon density wave spectroscopy, Chem Eng Technol 41 (6) (2018) 1139–1146, https://doi.org/10.1002/ceat.201700685.
[13] M. Sandmann, M. Münzberg, L. Bressel, O. Reich, R. Hass, Inline monitoring of high cell density cultivation of Scenedesmus rubescens in a mesh ultra-thin layer photobioreactor by photon density wave spectroscopy, BMC Res Notes 15 (1) (2022) 1–7, https://doi.org/10.1186/s13104-022-05943-2.
[14] B. Gutschmann, T. Schiewe, M.T.H. Weiske, P. Neubauer, R. Hass, S.L. Riedel, In-line monitoring of polyhydroxyalkanoate (PHA) production during high-cell-density plant oil cultivations using photon density wave spectroscopy, Bioengineering 6 (3) (2019), https://doi.org/10.3390/bioengineering6030085.
[15] R. Hass, O. Reich, Photon density wave spectroscopy for dilution-free sizing of highly concentrated nanoparticles during starved-feed polymerization, ChemPhysChem 12 (14) (2011) 2572–2575, https://doi.org/10.1002/cphc.201100323.
[16] R. Hass, M. Mnzberg, L. Bressel, O. Reich, Industrial applications of photon density wave spectroscopy for in-line particle sizing [invited], Appl Opt 52 (7) (2013) 1423–1431, https://doi.org/10.1364/AO.52.001423.
[17] Ö. Kutlug, R. Hass, S. Reck, A. Hartwig, Inline characterization of dispersion formation of a solvent-borne acrylic copolymer by photon density wave spectroscopy, Colloids Surf A Physicochem Eng Asp 556 (August) (2018) 113–119, https://doi.org/10.1016/j.colsurfa.2018.08.011.
[18] S. Schlappa, L.J. Brenker, L. Bressel, R. Hass, M. Münzberg, Process characterization of polyvinyl acetate emulsions applying inline photon density wave spectroscopy at high solid contents, Polymers (basel) 13 (4) (2021) 1–17, https://doi.org/10.3390/polym13040669.
[19] S. Schlappa, L. Bressel, O. Reich, M. Münzberg, Advanced Particle Size Analysis in High-Solid-Content Polymer Dispersions Using Photon Density Wave Spectroscopy, Polymers (Basel) 15 (15) (2023), https://doi.org/10.3390/polym15153181.
[20] L.I. Jacob, W. Pauer, Scale-up of emulsion polymerisation up to 100 L and with a polymer content of up to 67 wt%, monitored by photon density wave spectroscopy, Polymers (Basel) 14 (8) (2022), https://doi.org/10.3390/polym14081574.
[21] L.I. Jacob, W. Pauer, In-line monitoring of latex-particle size during emulsion polymerizations with a high polymer content of more than 60%, RSC Adv 10 (44) (2020) 26528–26534, https://doi.org/10.1039/d0ra02523b.
[22] L. Bressel, J. Wolter, O. Reich, Particle sizing in highly turbid dispersions by photon density wave spectroscopy: bidisperse systems, J Quant Spectrosc Radiat Transf 162 (2014) 213–220, https://doi.org/10.1016/j.jqsrt.2015.01.025.
[23] J. Gregory, Turbidity fluctuations in flowing suspensions, J Colloid Interface Sci 105 (2) (1985) 357–371, https://doi.org/10.1016/0021-9797(85)90309-1.
[24] I. de F. A. Mariz, I.S. Millichamp, J.C. de la Cal, J.R. Leiza, High performance water-borne paints with high volume solids based on bimodal latexes, Prog Org Coat 68 (3) (2010) 225–233, https://doi.org/10.1016/j.porgcoat.2010.01.008.
[25] I. de F. A. Mariz, J.R. Leiza, J.C. De la Cal, Competitive particle growth: a tool to control the particle size distribution for the synthesis of high solids content low viscosity latexes, Chem. Eng. J. 168 (2) (2011) 938–946, https://doi.org/10.1016/j.cej.2011.02.023.
[26] F. Chu, A. Guyot, High solids content latexes with low viscosity, in: University of the Basque Country (UPV/EHU), 2001, https://doi.org/10.1007/s003960000431.
[27] A. Guyot, F. Chu, M. Schneider, C. Graillat, T.F. McKenna, High solid content latexes, Progress in Polymer Science (oxford) 27 (8) (2002) 1573–1615, https://doi.org/10.1016/S0079-6700(02)00014-X.
[28] M. Schneider, C. Graillat, A. Guyot, T.F. McKenna, High solids content emulsions. III. Synthesis of concentrated latices by classic emulsion polymerization, J Appl Polym Sci 84 (10) (2002) 1916–1934, https://doi.org/10.1002/app.10513.
[29] S. Boutti, C. Graillat, T.F. McKenna, New routes to high solid content latexes: a process for in situ particle nucleation and growth, Macromol Symp 206 (2004) 383–398, https://doi.org/10.1002/masy.200450230.
[30] O. Elizalde, G.P. Leal, J.R. Leiza, Particle size distribution measurements of polymeric dispersions: a comparative study, Part. Part. Syst. Char. (2000) 236–243.